Article:

Black, BA, Lamarque, J-F, Marsh, DR orcid.org/0000-0001-6699-494X et al. (2 more authors) (2021) Global climate disruption and regional climate shelters after the Toba supereruption. Proceedings of the National Academy of Sciences, 118 (29). e2013046118. ISSN 0027-8424

https://doi.org/10.1073/pnas.2013046118

Appendix 1. Supplementary tables and figures

Table S1. List of simulations and boundary conditions.

Run numbers	**SO_2 emissions**	**Time of year**	**Emissions altitude**	**Duration**
Control	—	—	—	20 years
7	2000 Tg SO_2	June	18-25 km	10 years
8	2000 Tg SO_2	Dec.	18-25 km	10 years
9, 21-24	200 Tg SO_2	June	18-25 km	10 years
25-29	200 Tg SO_2	Dec.	18-25 km	10 years
16, 30-33	2000 Tg SO_2	Dec.	35-40 km	10 years
35-39	2000 Tg SO_2	June	35-40 km	10 years
40-44	2000 Tg SO_2	Sept.	35-40 km	10 years
50-54	2000 Tg SO_2	March	35-40 km	10 years
100-104	200 Tg SO_2	June	35-40 km	10 years
105-109	200 Tg SO_2	Dec.	35-40 km	10 years

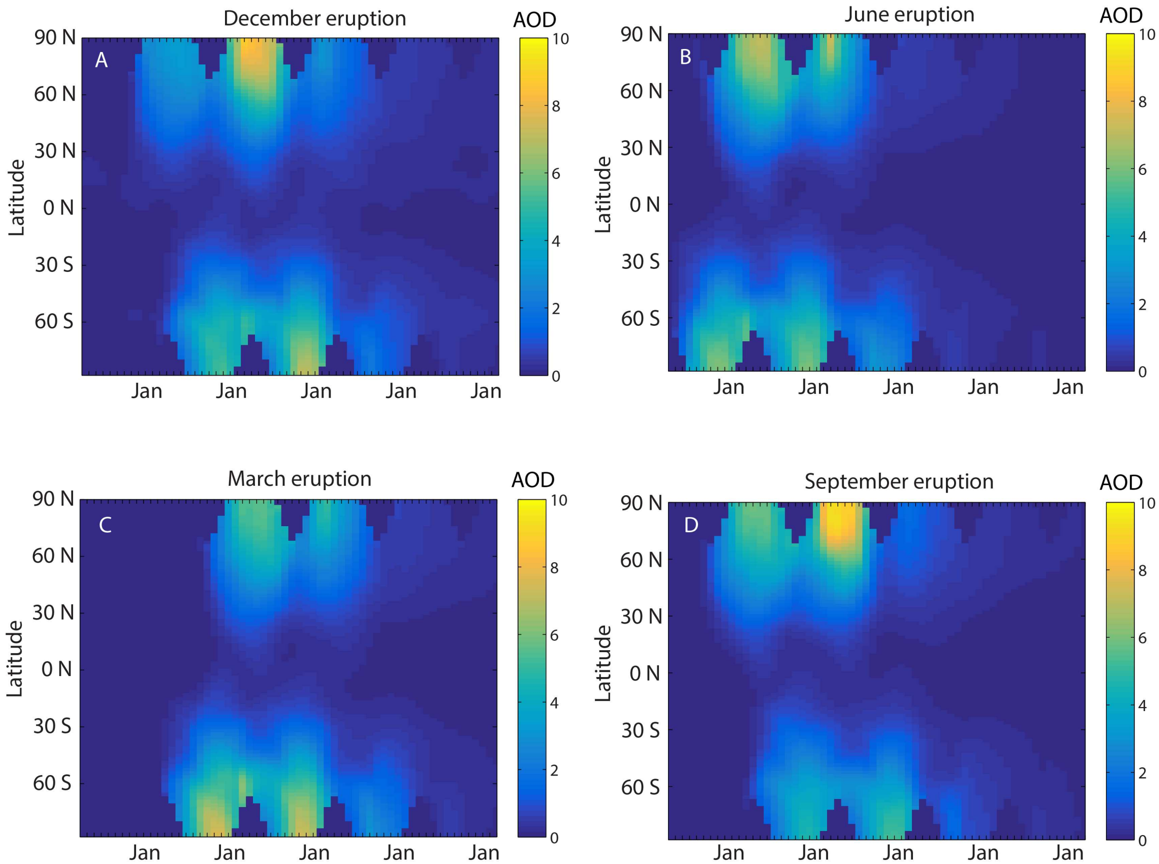

Figure S1. Evolution of zonally averaged aerosol optical depth (AOD, total aerosol optical depth in the visible band) for 2000 Tg SO_2 eruptions at different times of year. Each panel shows the mean of five ensemble members.

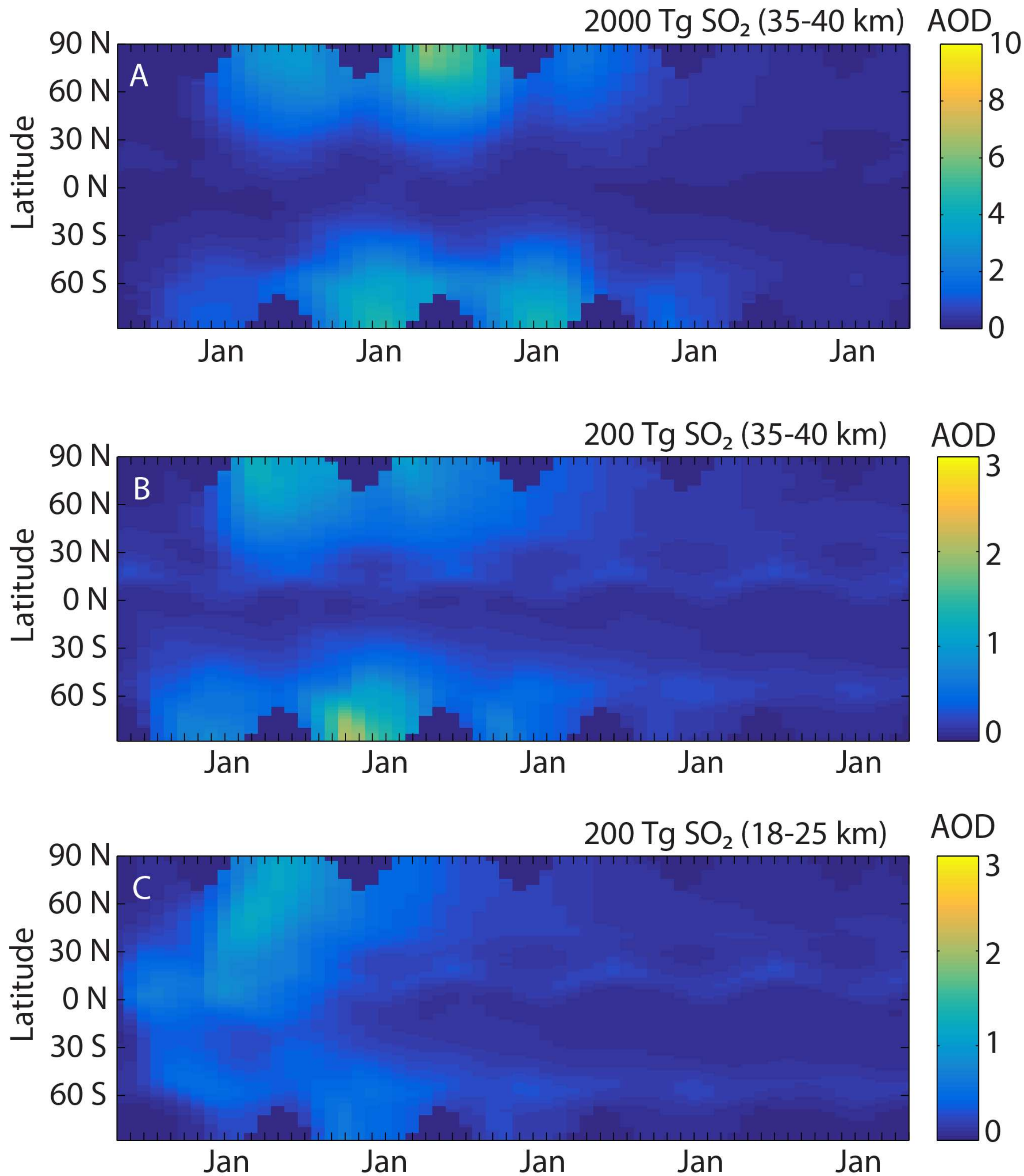

Figure S2. Zonally averaged aerosol optical depth (AOD) for (A) ensemble mean of 20 members with 2000 Tg SO_2 B) ensemble mean of 10 members with 200 Tg SO_2 (35-40 km emissions), or (C) ensemble mean of 10 members with 200 Tg SO_2 (18-25 km emissions) .

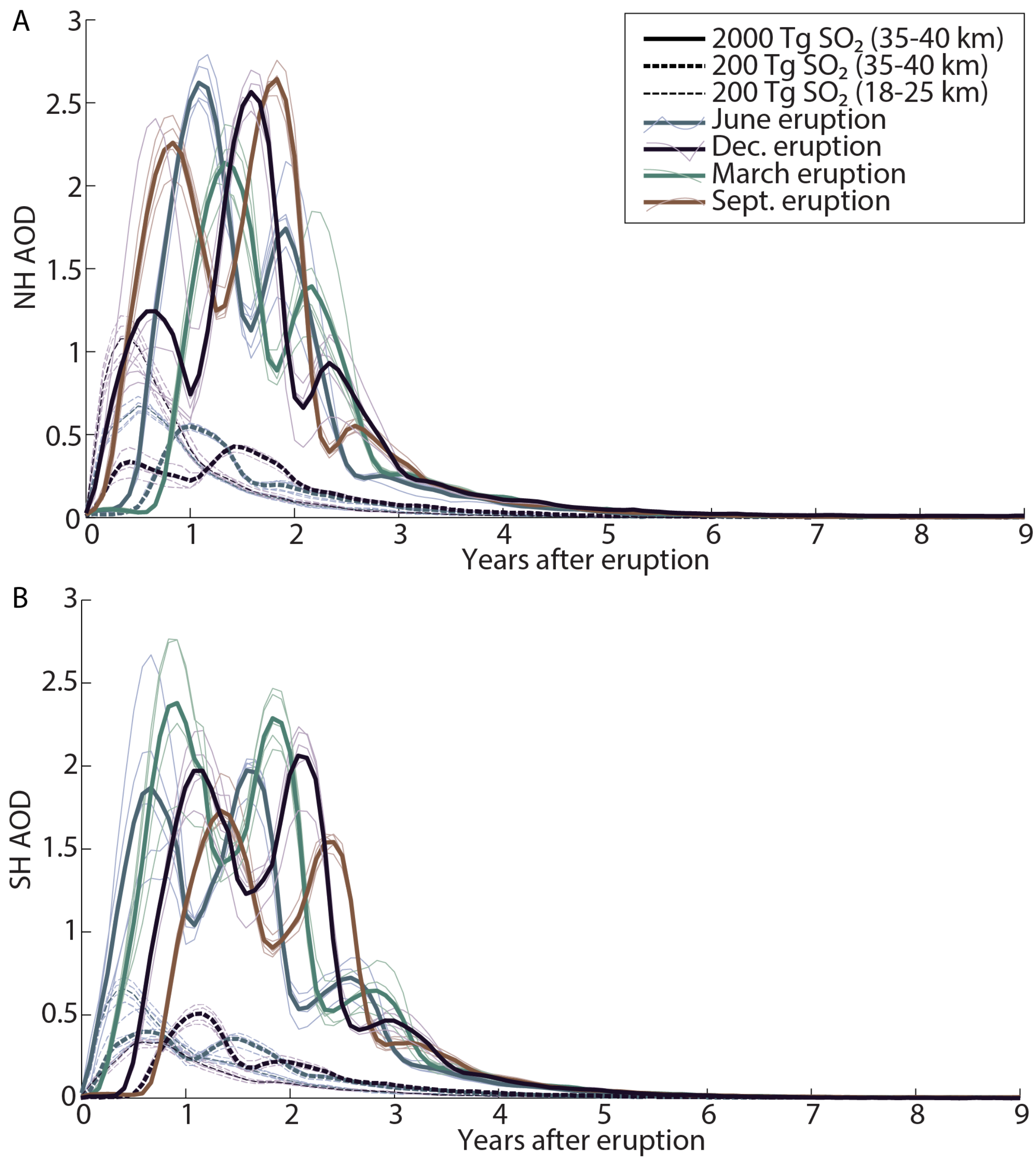

Figure S3. Hemispherically averaged aerosol optical depth (AOD) for 2000 Tg SO_2 or 200 Tg SO_2 emissions, sorted by eruption month. A) Northern hemisphere. B) Southern hemisphere. Light lines represent individual simulations, heavy lines represent ensemble means.

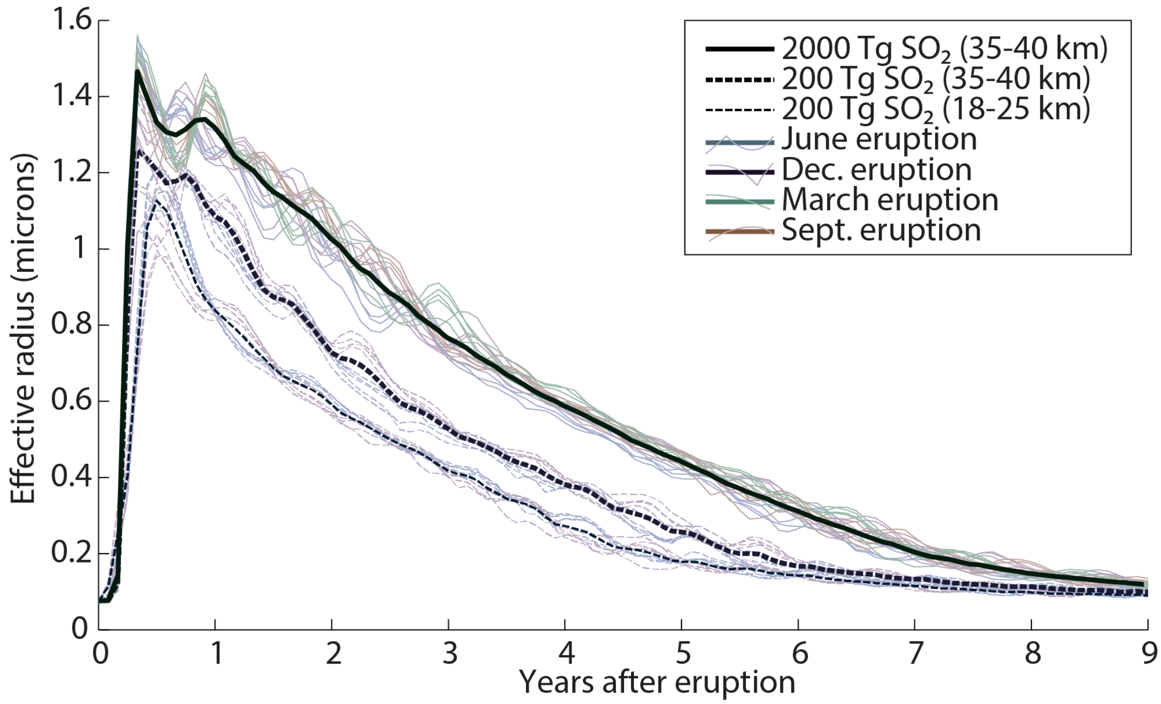

Figure S4. Evolution of global mean aerosol effective radius in the lower stratosphere (at 100 hPa). See also (22) for more detailed analysis and discussion of the evolution of aerosol effective radius following a large, tropical explosive eruption.

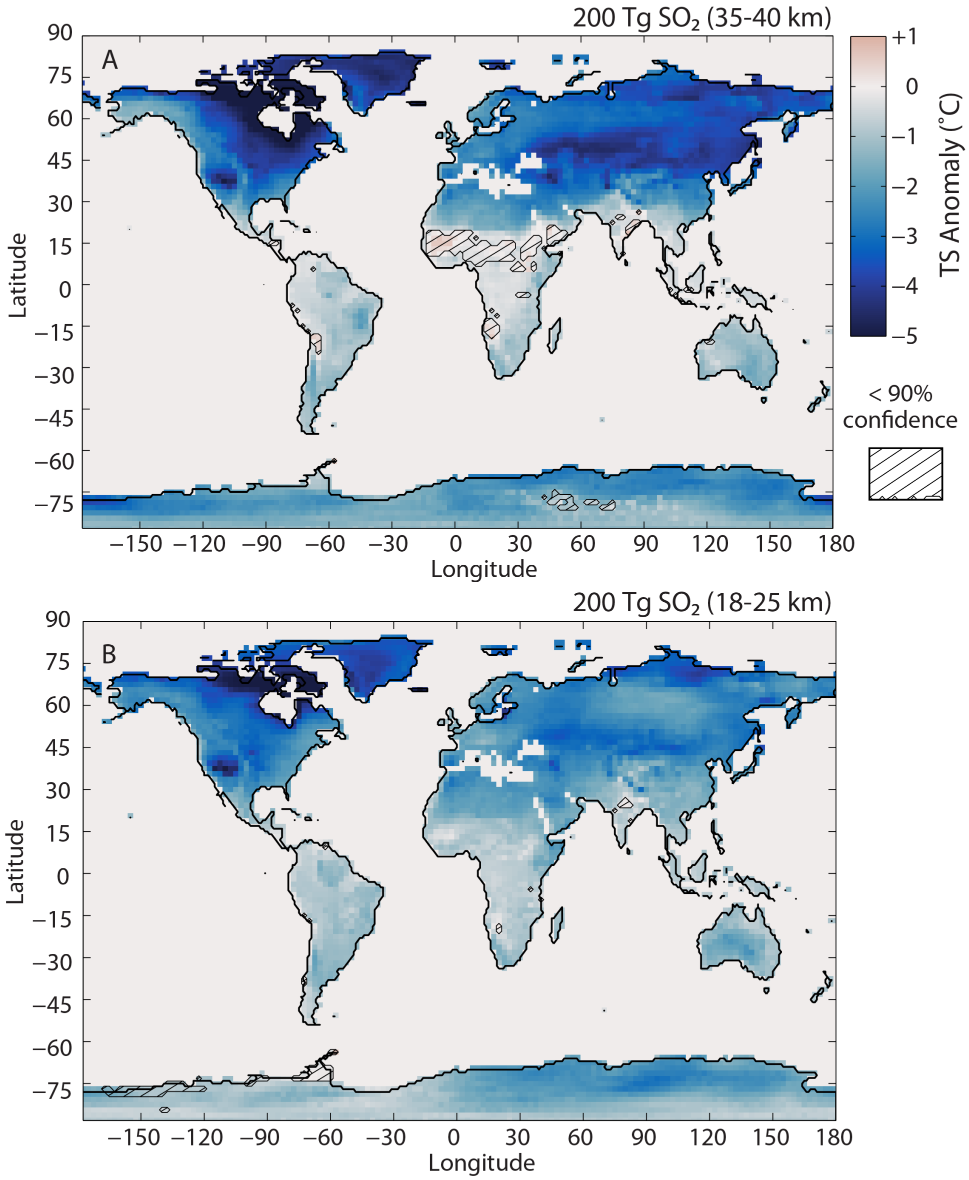

Figure S5. Global land surface temperature anomaly following the 200 Tg SO_2 Toba eruption scenario represented as the mean of the second year after an eruption over 10 ensemble members, which vary in the initial conditions. Cross-hatched areas indicate temperature anomalies that are not significant at the 90% level as determined with a Wilcoxon ranked sum test, compared with a monthly climatology from a 20-year control simulation. (A) shows 18-25 km altitude emissions, (B) shows 35-40 km altitude emissions.

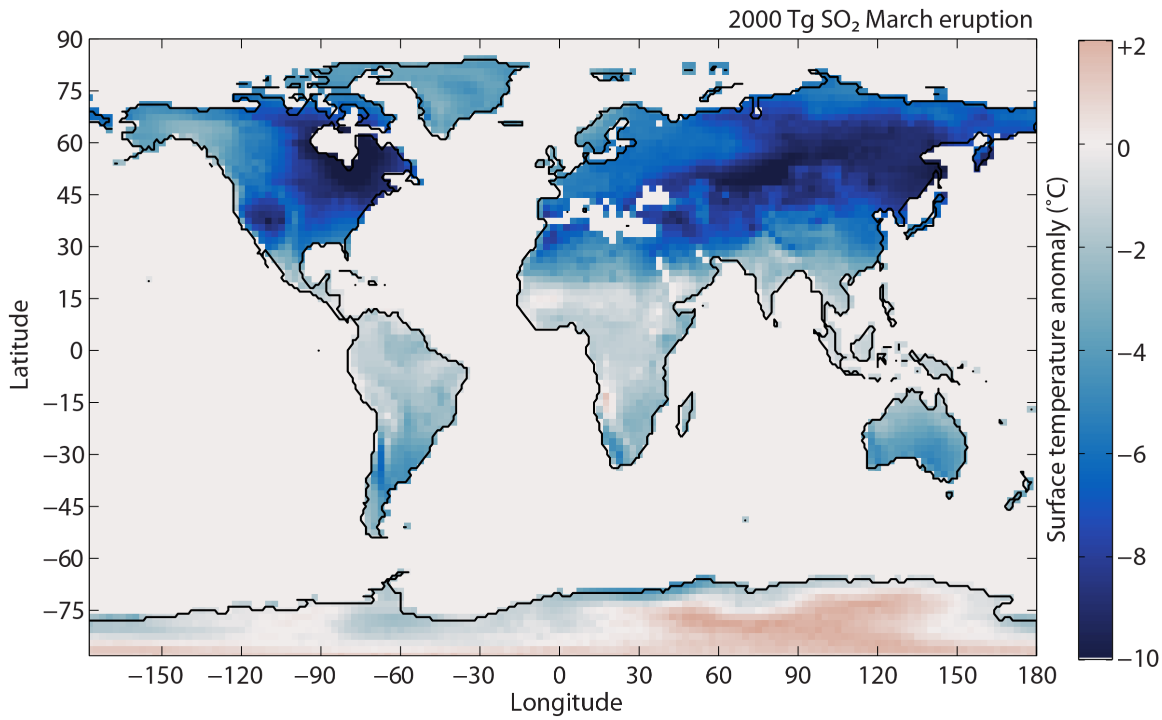

Figure S6. Surface temperature anomaly in the second year following 2000 Tg SO_2 simulations with the eruption in March, the ensemble with the largest proportion of the aerosol cloud in the southern hemisphere (Figure S3), showing that cooling in this scenario remains stronger in the northern Hemisphere, with relatively sheltered climate in southern Africa.

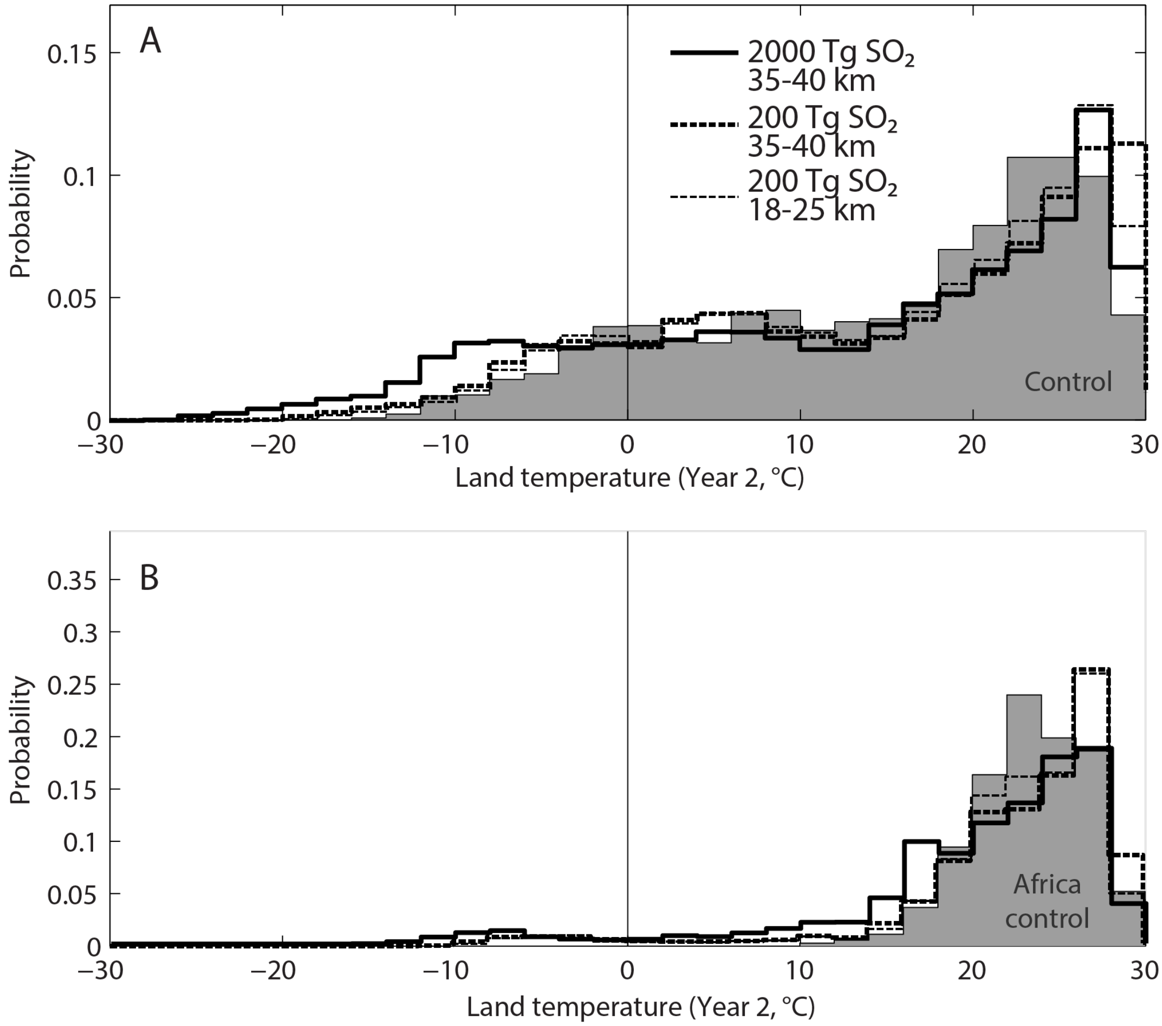

Figure S7. Probability distributions for monthly land temperatures based on a climatology from a 20-year control run and Toba emissions scenarios. (A) Global land temperatures from 60 °S to 60 °N. (B) Land temperatures in Africa.

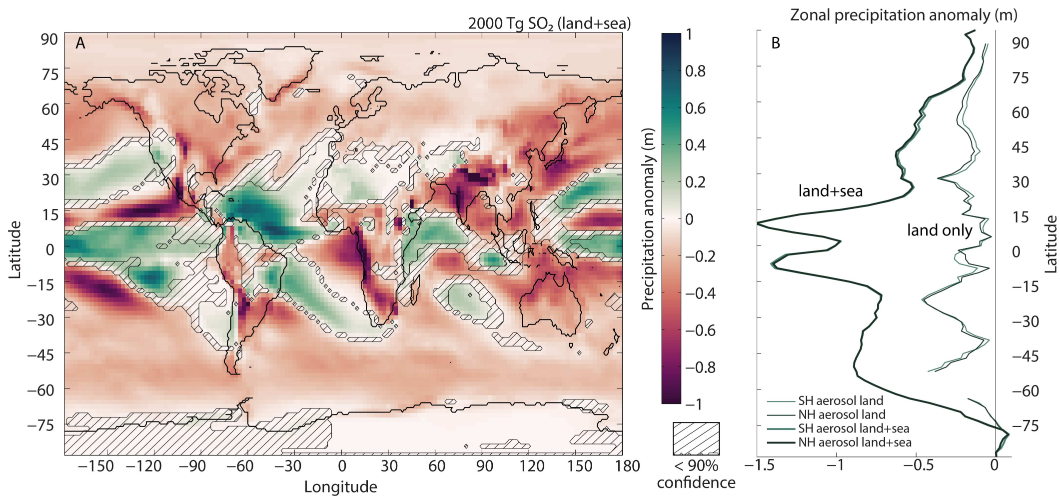

Figure S8. (A) Global and (B) zonal mean precipitation anomaly in the second year following an eruption. Panel a shows mean of all 2000 Tg SO_2 simulations and panel B shows zonal mean of the March and December eruption ensembles, which have aerosols weighted towards the southern and northern hemispheres respectively (Figure S3).

References

1. English JM, Toon OB & Mills MJ (2013) Microphysical Simulations of Large Volcanic Eruptions: Pinatubo and Toba. *Journal of Geophysical Research: Atmospheres* 118(4): 1880-1895.